electronics

MDPI

Article

Non-Singular Terminal Sliding Mode Controller with Nonlinear Disturbance Observer for Robotic Manipulator

Keyou Guo, Peipeng Shi *, Pengshuo Wang, Chengbo He and Haoze Zhang

School of Artificial Intelligence, Beijing Technology and Business University, Beijing 100048, China
* Correspondence: 2130061009@st.btbu.edu.cn

Abstract: Aiming at the problems of model uncertainties and other external interference in trajectory tracking control of n-degree of freedom manipulators, a non-singular terminal sliding mode controller with nonlinear disturbance observer (NDO–NTSMC) trajectory tracking method is proposed. A nonlinear disturbance observer (NDO) is designed to forecast and compensate the system external interference, and a nonlinear gain is designed to make the observer error achieve the expected exponential convergence rate so that the feedforward compensation control is realized. Then, a non-singular terminal sliding mode controller (NTSMC) built on nonlinear sliding surface is designed to surmount the singularity fault of classic terminal sliding mode controller (TSMC). Therefore, the time required from any initial state to reach the equilibrium point is finite. In addition, the redesign of the sliding surface ensures the tracking accuracy rate of uncertain systems. Then, based on Lyapunov principle, we complete the stability analysis. Finally, the method is applied to a 2-DOF robotic manipulator model compared with other methods. In the simulation, the manipulator needs to track a continuous trajectory under the condition of joint friction disturbance. The simulation result shows that the torque output of the designed method is chattering-free and smooth, and the tracking effect is precise. Simulation results indicate that the proposed controller has the advantages of excellent tracking performance, strong robustness, and a fast response.

Keywords: robotic manipulator; trajectory tracking; disturbance observer; sliding mode control; finite time convergence

Citation: Guo, K.; Shi, P.; Wang, P.; He, C.; Zhang, H. Non-Singular Terminal Sliding Mode Controller with Nonlinear Disturbance Observer for Robotic Manipulator. *Electronics* **2023**, *12*, 849. https://doi.org/10.3390/electronics12040849

Academic Editor: Sung Jin Yoo

Received: 2 December 2022
Revised: 4 January 2023
Accepted: 13 January 2023
Published: 8 February 2023

1. Introduction

As the robotic manipulator becomes increasingly significant in industry and research, perfect precision for trajectory tracking in these works has become an attractive research topic in recent years. The trajectory tracking of manipulators is one of the most important and difficult problems in the field of manipulator control. As a typical nonlinear and highly coupled MIMO system, the control of the manipulator not only plays an important role in practical application, but also has a significant impact on the control theory of similar MIMO systems. However, there are unknown variables including payload variation, time-varying joint friction, and external disturbance, which makes it difficult for the manipulators to achieve precise trajectory tracking control. In addition, the parameter variation and interference of the control system also have an adverse effect on the tracking control performance of the manipulator. To solve the trajectory tracking difficulties, a lot of advanced control techniques have been applied, such as feedback linearization [1], model predictive control [2], PID control [3], robust control [4], output adaptive control [5], classic sliding control [6–10], fuzzy control [11], and neural network control [12,13]. In these control methods, sliding mode control (SMC) [14,15] is recognized as an efficient and robust method, which can deal with nonlinear systems with bounded external interference and substantial uncertainties.

In traditional sliding mode control, a linear sliding surface is used. By designing the sliding mode surface, sliding mode control divides the system into the initial approaching

movement to the surface and the sliding mode movement in the surface. According to the system current state, it switches system state constantly to force the system trajectory as expected. Although it is extensively applied in the motion control of nonlinear systems, there exists two main disadvantages: chattering problems and sensitivity to the noise. Though the system state eventually approaches the given trajectory, the chattering phenomenon exists in its movement towards the equilibrium point. In addition, the final steady-state error cannot reduce to 0 in a limit time. To overcome this problem, Man et al. [16] proposed a terminal sliding mode (TSMC) built on a nonlinear sliding mode surface so that the system state variables could converge in a limited time. However, this method had the singularity problem and could not suppress the chattering phenomenon. Considering this issue, non-singular terminal sliding mode (NTSMC) was proposed [17–19]. By selecting fractional parameters in the control laws, this new control approach overcomes the singular problem. The sliding mode control system has the advantages of simplicity and robustness, but the chattering phenomenon cannot be fundamentally eliminated due to its own switching characteristics. Moreover, this control method is essentially a model-based control method, but in the actual control of the robotic manipulator system, the system uncertainty depends on the real-time system states and system inputs. Its dynamics model is very complicated and uncertain, which makes it difficult for the control system to achieve precise tracking using only a single sliding mode method. Considering this aspect of the problem, various advanced control methods combining sliding mode control were previously studied. Yagiz et al. [20] proposed a terminal fuzzy sliding mode control strategy applied to the manipulator. In the work [21], Jouila et al. combined terminal sliding mode and RBF neural network control to approach the model of the manipulator. However, these control methods combined with intelligent control are computationally expensive to be applied to real-time due to their complex design, parameter adjustment, or large amount of training. In addition, these methods cannot estimate and compensate for the disturbance. In order to strengthen the anti-disturbance ability, various disturbance rejection control methods have been extensively studied. To eliminate the system parameter perturbation, model uncertainties, and external disturbance, Chen et al. [22–25] designed a nonlinear disturbance observer and applied it to a 2-DOF rigid robotic arm system. Han [26] combined a disturbance observer with a terminal sliding mode controller (DO–TSMC), and put forward a finite time convergence of robotic arm sliding mode control method. Zhu [27] proposed a new sliding mode controller based on extended state observation (PD–ESO–SMC), which can realize real-time error measurement and compensation of interference without relying on the precise model.

In this paper, we establish a new non-singular terminal sliding mode controller with nonlinear disturbance observer (NDO–NTSMC) for manipulators. The major benefits of this article are summarized as follows:

The development of a non-singular terminal sliding mode controller with a nonlinear disturbance observer tracking method, which takes the place of the discontinuous sign function with the estimate of model uncertainties to avoid the chattering problem. It also can be applied to observe and compensate external disturbance.

The superiority of the raised tracking control method is confirmed by comparing the simulation experimental results of a 2-DOF manipulator with (1) non-singular terminal sliding mode control method without observer (NTSMC) and (2) classical PD controller with disturbance observer (NDO–PD).

The rest of this article is organized as follows: the dynamics model of the n-DOF rigid robotic manipulators system is establishment in Section 2. Then, in Section 3, a nonlinear disturbance observer is developed to manipulate the problem of external interference. In addition, the system controller is built up with the non-singular terminal sliding mode method. Next in Section 4, we discuss the stability of the controller designed above. We illustrate the satisfactory performance of the proposed method by providing several numerical contrast simulations in Section 5, which apply the control strategy to a 2-DOF

robotic manipulator system. Lastly, conclusions and further extensions are presented in Section 6.

2. The Dynamics Model of n-DOF Robotic Manipulators

For the n-degree of freedom rigid robotic manipulator, considering the model indeterminacy, parameter change, and other external disturbances, the general form of the dynamics established by the Lagrange method is as follows:

$$(M_0(q) + \Delta M(q))\ddot{q} + (C_0(q,\dot{q}) + \Delta C(q,\dot{q})) + (G_0(q) + \Delta G(q)) = \tau + \rho(\dot{q}) + d(t) \quad (1)$$

where $M_0(q) \in \mathbb{R}^{n\times n}$ is the nominal positive inertia matrix, $C_0(q,\dot{q}) \in \mathbb{R}^{n\times 1}$ denotes the nominal centrifugal–Coriolis matrix. $G_0(q) \in \mathbb{R}^{n\times n}$ is the gravity nominal vector. $\Delta M(q)$, $\Delta C(q,\dot{q})$, and $\Delta G(q)$ for the model indeterminacy. $\tau \in \mathbb{R}^n$ is the joint input torque. $\rho(q) \in \mathbb{R}^n$ is the joint friction torque. $q, \dot{q}, \ddot{q} \in \mathbb{R}^n$ are on behalf of the joint's position, angular velocity, and angular acceleration, respectively. $d(t) \in \mathbb{R}^n$ is the unknown external interference torque. According to (1), the dynamic function of the manipulators is replaced as follows:

$$M(q)\ddot{q} + C(q,\dot{q}) + G(q) = \tau + f(q,\dot{q}) \quad (2)$$

where $f(q,\dot{q}) = -(\Delta M\ddot{q} + \Delta C + \Delta G) + \rho(\dot{q}) + d(t)$ is defined as the total interference, which the disturbance observer aims to estimate the observable part. The other invisible part can be compensated by the sliding mode controller. For the dynamic model matrices $M(q)$ and $C(q,\dot{q})$, there are some properties that hold:

Property 1. *The matrix $M(q) \in \mathbb{R}^{n\times n}$ is positive definite and symmetric;*

Property 2. *The matrix $(M(q) - 2C(q,\dot{q}))$ is skew symmetric.*

Define the tracking error $e, \dot{e}$:

$$\begin{cases} e = q - \dot{q}_d \\ \dot{e} = \dot{q} - \dot{q}_d \end{cases} \quad (3)$$

where q_d is the desired trajectory position of the joint.

Considering the subsequent control strategy, we made the following assumptions in this article:

Assumption 1. The actual angular position q and velocity q of the manipulator joints are measurable, continuous, and bounded;

Assumption 2. Total disturbance f is continuously differentiable, it is assumed to be unknown but bounded and its upper bound defined as $\|f\| < \Gamma$.

3. Control Design

The objective of the controller is to converge the tracking error e in a finite time. The structure drawing of the control system is shown below in Figure 1, which mainly consists of the following parts: (1) The disturbance observer is set to carry out real-time estimation and torque compensation for the observable part of the total interference. The actual torque input of the manipulator is the corrected control torque; (2) d the nonsingular terminal sliding mode surface is designed. The equivalent input τ_0 and uncertainty compensation u_1, u_2 are determined as:

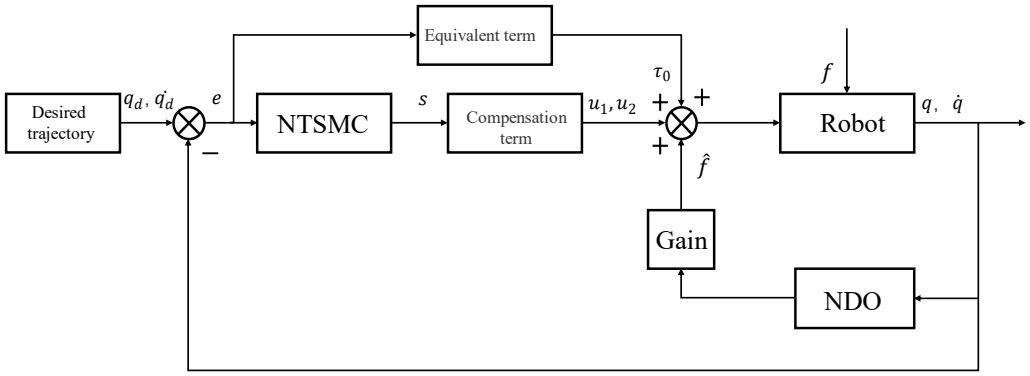

Figure 1. Control system structure.

3.1. Disturbance Observer Design

According to Equation 2, a robotic manipulator system is highly nonlinear and has strong coupling. Therefore, it is very difficult to realize decoupling by establishing an accurate dynamics model, especially in the case of external disturbance, modeling errors, and parameter perturbation. Think of the external disturbance as one part so that we can use the nonlinear disturbance observer (NDO) to evaluate it. The principle is to use the D-value between the estimate output and the real-time output to correct the estimate value. Thus, the disturbance observer is defined as:

$$\dot{\hat{f}} = -L(q,\dot{q})\hat{f} + L(q,\dot{q})(M(q)\ddot{q} + C(q,\dot{q}) + G(q) - \tau) \tag{4}$$

$\hat{f}$ denotes the derivative of the disturbance observation, $L(q,\dot{q}) \in \mathbb{R}^{n\times n}$ is the observation gain matrix, and the observer error is defined as $\zeta = f - \hat{f}$, then $\dot{\zeta} = \dot{f} - \dot{\hat{f}}$. Due to the observational noise, it is hard to obtain the acceleration information from the differential signal in practice, but the angular acceleration value of the state is required, so the nonlinear observer is further designed by these following steps:

Step 1

Firstly define the auxiliary parameter vector:

$$z = \hat{f} - p(q,\dot{q}) \tag{5}$$

where $z \in \mathbb{R}^n$ denotes the parameter vector showing the observer state, $p(q,\dot{q})$ is the function vector to be defined, which has the following nonlinear relationship with the observation gain matrix $L(q,\dot{q})$:

$$L(q,\dot{q})M(q)\ddot{q} = \frac{dp(q,\dot{q})}{dt} \tag{6}$$

Step 2

Invoking (5) and (6), the structure of the NDO can be obtained:

$$\begin{cases} \dot{z} = -L(q,\dot{q})z + L(q,\dot{q})(C(q,\dot{q}) + G(q) - \tau) \\ \hat{f} = z + p(q,\dot{q}) \end{cases} \tag{7}$$

where it is given by Equation (6).

Step 3

From the function of observer error $\dot{\zeta} = \dot{f} - \dot{\hat{f}}$, it is assumed that it changes slowly with respect to the dynamic characteristics of the observer, thus, $\dot{f} = 0$. Following from (5)–(7), the observer error equation:

$$\dot{\zeta} + L(q,\dot{q})\zeta = 0 \tag{8}$$

Theorem 1. *When the NDO designed for the robotic manipulators control system adopts the structure shown in Equation (7) and the observer error is Equation (8), the asymptotically stability of the observer can be guaranteed. Moreover, it can be selected to reach the expected exponential convergence rate. According to reference [24], the Lyapunov convergence proof of this theory is as follows.*

Proof of Theorem 1. Define the nonlinear observation gain matrix $p(q, \dot{q})$ as:

$$\frac{dp(q,\dot{q})}{dt} = r\widetilde{\gamma}^{-1}\ddot{q} \tag{9}$$

where $\widetilde{\gamma}^{-1} \in \mathbb{R}^{n\times n}$ is a invertible matrix. Combine Equations (6) and (10) to obtain the nonlinear observation gain matrix $L(q, \dot{q})$:

$$L(q,\dot{q}) = r\widetilde{\gamma}^{-1}M(q)^{-1} \tag{10}$$

According to Property 1, a matrix $\overline{M}(q)$ must exist that satisfies the condition:

$$M(q) = (\widetilde{\gamma}^{-1})^{T}\overline{M}(q)\widetilde{\gamma}^{-1} \tag{11}$$

meaning that

$$M(q)^{-1} = \widetilde{\gamma}\overline{M}(q)\widetilde{\gamma}^{-1} \tag{12}$$

By inserting (12) into (10), we obtain:

$$L(q,\dot{q}) = r\overline{M}(q)^{-1}\widetilde{\gamma}^{-1} \tag{13}$$

It is obvious that $\overline{M}(q)$ is positive definite. Define the Lyapunov function:

$$V(e,q) = e^{T}\overline{M}(q)e \tag{14}$$

By deriving and simplifying the equation, we can see:

$$\frac{dV(e,q)}{dt} = -e[r\gamma^{T} + r\gamma - \overline{M}(\dot{q})]e \tag{15}$$

In order to ensure that matrix V is negative definite ($dV < 0$), the principal minors of each order of matrix $[r\gamma^{T} + r\gamma - \overline{M}(\dot{q})]$ are required to be greater than 0. This condition can be satisfied by designing matrix γ. Also, the global asymptotic stability of the observer at the equilibrium point ($e = 0$) can be guaranteed. Assume that k_1 is the minimum eigenvalue of $\overline{M}(q)$ for all the positions q, and k_2 is the maximum.

Hence:

$$\frac{dV(e,q)}{dt} \leq -k_1\|e\|^2 \tag{16}$$

$$V(e,q) = e^{T}\overline{M}(q)e \leq k_2 e^{T}e = k_2\|e\|^2 \tag{17}$$

Combine the two equations:

$$\frac{dV(e,q)}{dt} \leq -k_2\frac{k_1}{k_2}\|e\|^2 \leq -\frac{k_1}{k_2}V(e,q) \tag{18}$$

Calculate the definite integral. Therefore, the convergence rate of the observer is:

$$V(t) \leq V(t_0)e^{-(k_1/k_2)(t_1-t_0)} \tag{19}$$

The convergence speed is bounded by k_1/k_2. However, for a robotic manipulator, k_2 is fixed. Therefore, it can be achieved by selecting the function gain r to reach the desired exponential convergence rate.

If the feedforward gain matrix of the observer in Figure 1 is selected as the unit matrix, the system dynamics Equation (2) becomes:

$$\ddot{q} = M(q)(\tau + f(q,\dot{q}) - \hat{f}(q,\dot{q}) - C(q,q) - G(q)), \tag{20}$$

which yields:

$$\ddot{q} = M(q)^{-1}(\tau + \zeta - C(q,\dot{q}) - G(q)) \tag{21}$$

After the compensation, the disturbance force is reduced from f to ζ, which can effectively reduce the disturbance torque and suppress chattering. □

3.2. Non-Singular Terminal Sliding Mode Controller Design

To solve singularity difficulties caused by TSMC, the non-singular terminal sliding mode function is defined as:

$$s = e + C_1 \dot{e}^{\beta/\alpha} \tag{22}$$

where $C_1 = diag[c_{11}c_{12}\ldots c_{1n}]$,$1 < \beta/\alpha < 2$,$\beta$, α are all positive odd numbers. The sliding surface is designed to:

$$\tau = \tau_0 + u_1 + u_2 \tag{23}$$

where:

$$\tau_0 = C(q,\dot{q}) + G(q) + M(q)\ddot{q}_d \tag{24}$$

$$u_1 = -\frac{\alpha}{\beta} M(q) {C_1}^{-1} diag(\dot{e}^{2-\beta/\alpha}) \tag{25}$$

$$u_2 = -\Gamma \cdot \frac{[s^T C_1 diag(\dot{e}^{\beta/\alpha-1}) M(q)^{-1}]^T \|s\|}{\left\| s^T C_1 diag(\dot{e}^{\beta/\alpha-1}) M(q)^{-1} \right\|^2} \times \left\| C_1 diag(\dot{e}^{\beta/\alpha-1}) M(q)^{-1} \right\| \tag{26}$$

where τ_0 represents the equivalent torque. u_1 is terminal convergence term. u_2 is compensation term. Γ is the upper bound of total disturbance, including observable parts such as joint friction and unobservable parts such as model uncertainty, parametric motion, and other unknown interferences, so it is defined as $\Gamma = \chi_0 + \chi_1\|q\| + \chi_2\|\dot{q}\|^2$, where χ_0, χ_1, χ_2 are unknown positive constants that relate to the real-time joint position.

4. Controller Stability

Theorem 2. *For the robotic manipulator in the form of Equation (11), the control law is selected in the form of Equation (13). In addition, the nonsingular terminal sliding surface shown in Equation (12) is used. The system is asymptotically stable.*

Proof of Theorem 2. Define Lyapunov function as:

$$\Lambda = \frac{1}{2} s^T \mathrm{s} \tag{27}$$

substituting (12) and (14) into (3), one obtains:

$$\begin{aligned}
\ddot{e}(t) &= \ddot{q} - \ddot{q}_d \\
&= M(q)^{-1}(\tau + \zeta - C(q,q) - G(q)) - \ddot{q}_d \\
&= M(q)^{-1}(\tau_0 + u_1 + u_2 + \zeta - C(q,q) - G(q)) - \ddot{q}_d \\
&= M(q)^{-1}(C(q,q) + G(q) + M(q)\ddot{q}_d + u_1 + u_2 + \zeta - C(q,q) - G(q)) - \ddot{q}_d \\
&= M(q)^{-1}(M(q)\ddot{q}_d + u_1 + u_2 + \zeta) - \ddot{q}_d \\
&= M(q)^{-1}(u_1 + u_2 + \zeta)
\end{aligned} \tag{28}$$

and according to (16), we can obtain:

$$\begin{aligned}
&\dot{e} + \tfrac{\beta}{\alpha} C_1 diag(\dot{e}^{\beta/\alpha - 1}) M(q)^{-1} u_1 \\
&= \dot{e} + \tfrac{\beta}{\alpha} C_1 diag(\dot{e}^{\beta/\alpha - 1}) M(q)^{-1} (-\tfrac{\alpha}{\beta} M(q) {C_1}^{-1} diag(\dot{e}^{2-\beta/\alpha})) \\
&= \dot{e} - diag(\dot{e}^{\beta/\alpha - 1}) diag(\dot{e}^{2-\beta/\alpha}) \\
&= 0
\end{aligned} \tag{29}$$

thereafter, by inserting (19) and (20) into (18), it is not difficult to calculate as:

$$\begin{aligned}
\dot{\Lambda} \quad &= s^T \dot{s} = s^T (\dot{e} + \tfrac{\beta}{\alpha} C_1 diag(\dot{e}^{\beta/\alpha - 1}) \ddot{e}) \\
&= s^T \left[\dot{e} + \tfrac{\beta}{\alpha} C_1 diag(\dot{e}^{\beta/\alpha - 1}) M(q)^{-1} (u_1 + u_2 + \zeta(q, \dot{q})) \right] \\
&= s^T \left[\tfrac{\beta}{\alpha} C_1 diag(\dot{e}^{\beta/\alpha - 1}) M(q)^{-1} (u_2 + \zeta(q, \dot{q})) \right] \\
&= s^T \left\{ \tfrac{\beta}{\alpha} C_1 diag(\dot{e}^{\beta/\alpha - 1}) M(q)^{-1} \cdot \left[-\Gamma \cdot \frac{\left[s^T C_1 diag(\dot{e}^{\beta/\alpha - 1}) M(q)^{-1} \right]^T ||s||}{||s^T C_1 diag(\dot{e}^{\beta/\alpha - 1}) M(q)^{-1}||^2} \times ||C_1 diag(\dot{e}^{\beta/\alpha - 1}) M(q)^{-1}|| + \zeta(q, \dot{q}) \right] \right\} \\
&= -\tfrac{\beta}{\alpha} ||s|| \cdot ||C_1 diag(\dot{e}^{\beta/\alpha - 1}) M(q)^{-1}|| \cdot (\chi_0 + \chi_1 ||q|| + \chi_2 ||\dot{q}||_2) + \tfrac{\beta}{\alpha} s^T C_1 diag(\dot{e}^{\beta/\alpha - 1}) M(q)^{-1} \cdot \zeta(q, \dot{q}) \\
&\le -\tfrac{\beta}{\alpha} ||s|| \cdot ||C_1 diag(\dot{e}^{\beta/\alpha - 1}) M(q)^{-1}|| \cdot (\chi_0 + \chi_1 ||q|| + \chi_2 ||\dot{q}||_2) + \tfrac{\beta}{\alpha} ||s^T|| \cdot ||C_1 diag(\dot{e}^{\beta/\alpha - 1}) M(q)^{-1}|| \cdot ||\zeta(q, \dot{q})|| \\
&= -\tfrac{\beta}{\alpha} ||s|| \cdot ||C_1 diag(\dot{e}^{\beta/\alpha - 1}) M(q)^{-1}|| \cdot [(\chi_0 + \chi_1 ||q|| + \chi_2 ||\dot{q}||_2) - ||\zeta(q, \dot{q})||] \\
&< 0 \qquad\qquad (||s||)
\end{aligned} \tag{30}$$

Eventually, as we can see, the Lyapunov derivative is negative, which means the system is asymptotically stable and theorem 1 is proved. Meanwhile, the tracking error index is $(\beta/\alpha - 1) > 0$, which solves the singularity difficulty of TSMC at the point when $e = 0, \dot{e} \neq 0$. From the function of the control law (14), the uncertainties compensation control item replaces the switching control item, and the chattering phenomenon is suppressed in this way.

5. Simulation Result

To test and verify the effectiveness and superiority of the above control algorithm, the redesigned control method is utilized to the tracking simulation of a 2-DOF robotic manipulator. The diagrammatic sketch is as shown in Figure 2. The physical parameters of the manipulator for simulation are shown in Table 1.

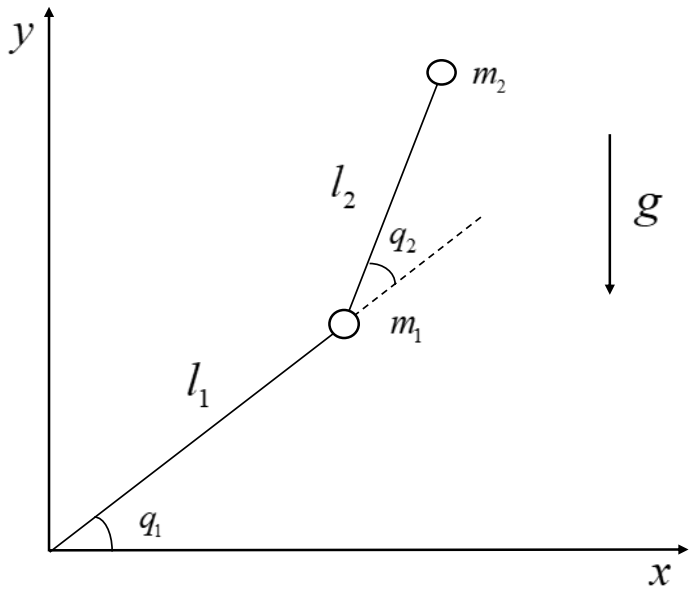

Figure 2. The robotic manipulator (2-DOF).

Table 1. Physical parameters of the robotic manipulator.

Symbols	Definition	Values
m_1	Mass: link 1	0.5 kg
m_2	Mass: link 2	1.5 kg
l_1	Length: link 1	1 m
l_2	Length: link 2	0.8 m
J_1	Moment of inertia: link 1	5 kgm^2
J_2	Moment of inertia: link 2	5 kgm^2
g	Acceleration due to gravity	9.81 m/s^2

The dynamic parameter matrix of the of the robotic manipulator are:

$$q = \begin{bmatrix} q_1 \\ q_2 \end{bmatrix}, \tau = \begin{bmatrix} \tau_1 \\ \tau_2 \end{bmatrix}$$

$$M(q) = \begin{bmatrix} m_{11} & m_{12} \\ m_{21} & m_{22} \end{bmatrix},$$
$$C(q, \dot{q}) = \begin{bmatrix} -m_2 l_1 l_2 \sin(q_2) \dot{q}^2{}_1 - 2 m_2 l_1 l_2 \sin(q_2) \dot{q}_1 \dot{q}_2 \\ m_2 l_1 l_2 \sin(q_2) \dot{q}_2^2 \end{bmatrix}$$

where:

$$m_{11} = (m_1 + m_2) l_1^2 + m_2 l_2^2 + 2 m_2 l_1 l_2 \cos(q_2) + J_1$$
$$m_{12} = m_{21} = m_2 l_2^2 + m_2 l_1 l_2 \cos(q_2)$$
$$m_{22} = m_2 l_2^2 + J_2$$

Consider the joint friction as the observable external disturbance, $\eta_{v1} = \eta_{v2} = 0.5$ N $\cdot$ m are viscous friction factors. $\mu_{c1} = \mu_{c2} = 10.0$ N $\cdot$ m are coulombic friction factors. Define the joint disturbance torques as:

$$\rho(t) = \begin{bmatrix} \rho_1 \\ \rho_2 \end{bmatrix} = \begin{bmatrix} \eta_{v1} \dot{q}_1 + \mu_{c1} \mathrm{sgn}(\dot{q}_1) \\ \eta_{v2} \dot{q}_2 + \mu_{c2} \mathrm{sgn}(\dot{q}_2) \end{bmatrix} \tag{31}$$

The desired trajectory signal is as follows:

$$q_d = \begin{bmatrix} q_{d1} \\ q_{d2} \end{bmatrix} = \begin{bmatrix} \sin(0.2\pi t) \\ \sin(0.2\pi t) \end{bmatrix} \tag{32}$$

The experiment simulation is developed by modeling in MATLAB/SIMULINK. The disturbance observer obtained in (6) and the nonsingular terminal sliding mode control shown in (13) are used. Then, the parameters used are chosen as follows: observer function vector gain $r = 250$. The feedforward gain matrix is taken as E_2. Nonsingular terminal sliding surface coefficient matrix $C_1 = \begin{bmatrix} 0.9 & 0 \\ 0 & 0.9 \end{bmatrix}$,$\beta = 5$, $\alpha = 3$, $\chi_0 = 10$, $\chi_1 = 20$, $\chi_2 = 30$. The simulation settings: differential equation solver is ode45. The simulation time is 10 s. The solution step is variable-step. The initial state of this system: joint angle $q_1(0) = q_2(0) = 0.5rad$, joint angular velocity $\dot{q}_1(0) = \dot{q}_2(0) = 0$.

To better test the superiority of the control system (NDO–NTSMC), we compare the two methods of non-singular terminal sliding mode controller without observer (NTSMC) and the classic PD controller with observers (NDO–PD), which are introduced as follows. All simulations are performed under the same simulation conditions.

NTSMC: In order to reflect the observer's ability to track external disturbance, and the performance improvement of the controller, in the NTSMC method, only NTSMC is tested. The control function and the sliding surface keep up with (13) and (14);

NDO–PD: To better show the tracking effect of the NTSMC, a PD controller based on the disturbance observer is developed. The PD control law is taken as:

$$\tau_{PD} = \begin{bmatrix} \tau_{PD1} \\ \tau_{PD2} \end{bmatrix} = \begin{bmatrix} k_P e_1 + k_D \dot{e}_1 \\ k_P e_2 + k_D \dot{e}_2 \end{bmatrix} \tag{33}$$

where the proportions and differential gains are $k_P = 400$, $k_D = 100$. For the disturbance observer, its parameter is consistent with NDO–NTSMC.

The simulation results are shown below. The observation effect of the disturbance observer on the joint friction is shown in Figure 3. The output torque of the controller is shown in Figure 4.

Figure 5 shows the tracking performance comparison effect. Finally, Figure 6 mainly shows the tracking error comparison result.

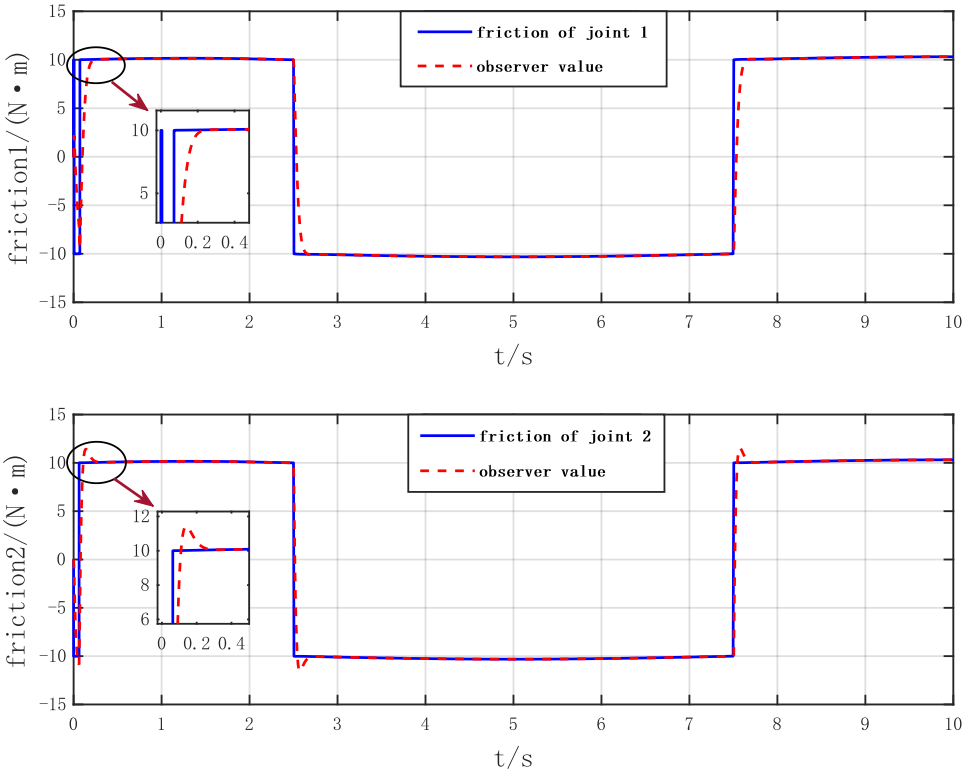

Figure 3. Observer output (The arrows point to the overshoot phenomenon).

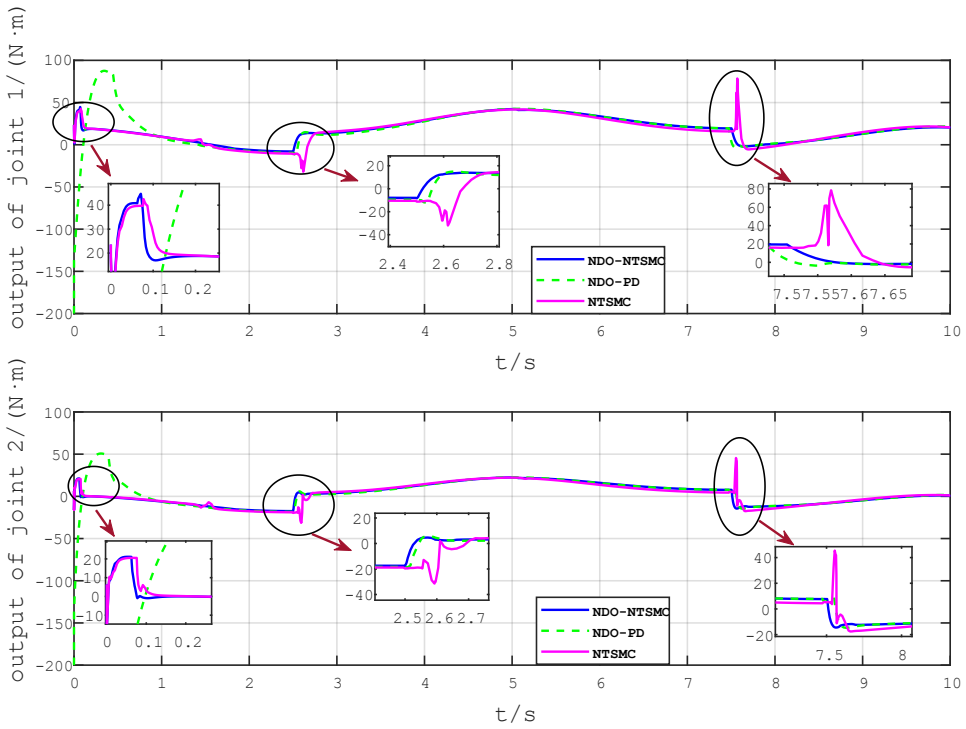

Figure 4. Controller output torque (with partial enlarged detail).

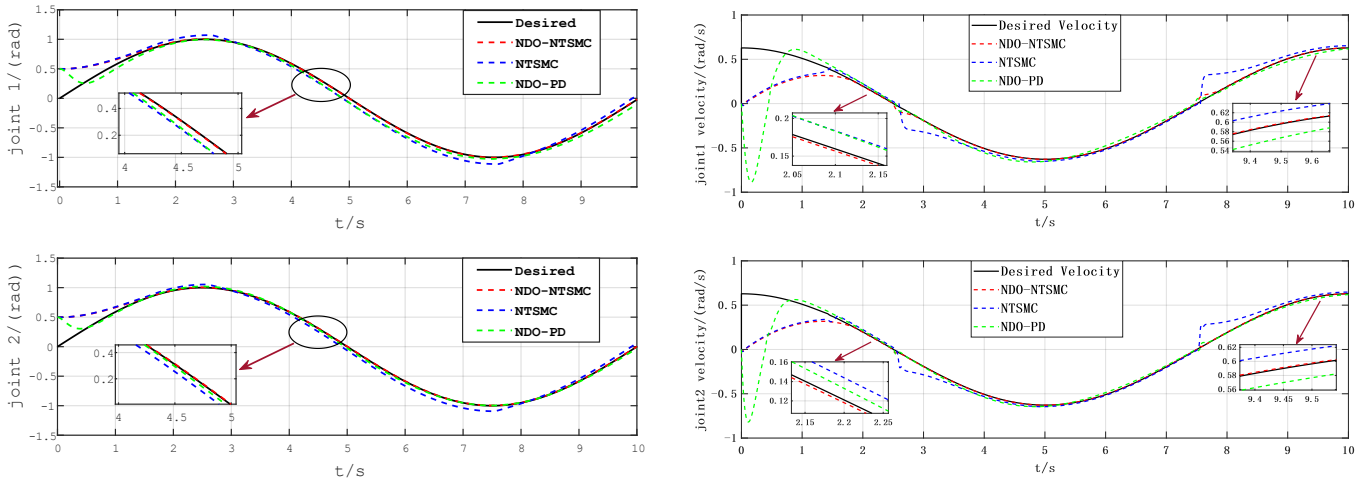

(**a**) (**b**)

Figure 5. Controller trajectory tracking effect: (**a**) position trajectory of joints; (**b**) velocity trajectory of joints (with partial enlarged detail).

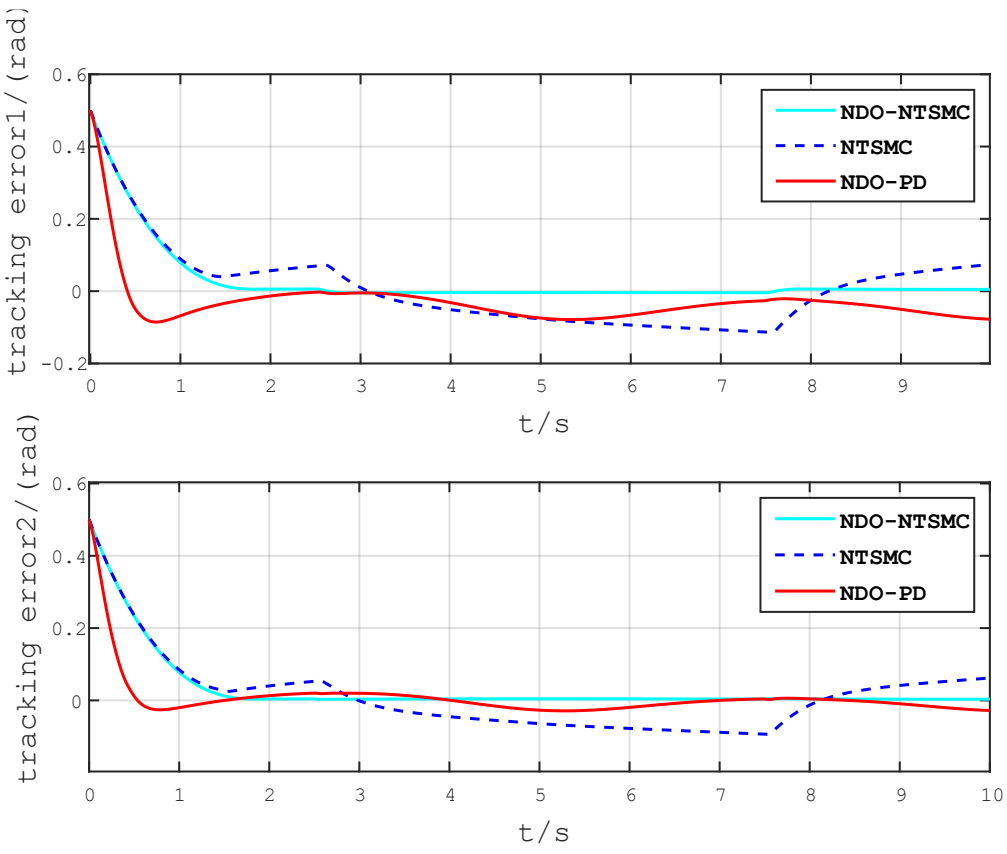

Figure 6. Controller trajectory tracking error.

It is discovered from Figure 3 that the joint friction simulates the external step disturbance signals, which is applied to the joints at 0.062 s and lasts for about 2.441 s. Though the amplitude of the disturbance accounts for about 20% of the amplitude of the controller output, the observer still has a fast response speed (0.175 s) and a small overshoot (13.5%), which shows that the designed observer has a good effect on tracking time-varying external disturbances.

From the comparison result of the output torque of the three controllers in Figure 4, the NDO–NTSMC responds quickly to disturbances such as joint rotation direction change and interference torque. Additionally, the output torque is smooth and chattering-free, which shows that it can effectively compensate for these challenges. From the local magnification, the NTSMC output torque

has obvious chattering phenomenon when the direction of joint rotation changes (at 2.5 s, 7.5 s). The NDO–PD controller output saturates at beginning, but the output of the NDO–NTSMC converges faster and the overshoot is smaller. It shows that NTSMC performance is better when the model is inherently nonlinear.

Figures 5 and 6 show the tracking performance result of the controller system. From Figure 5, the trajectory tracking effect of NDO–NTSMC converges faster in position and velocity tracking. The system has better anti-interference with the disturbance observer. The controller NDO–PD responds fast at the initial moment, but, at the same time, the amplitude of the output is too large to produce an overshoot phenomenon. Furthermore, there is a large steady-state error after stabilization. In Figure 6, we can see this in more detail. Compared with the other two controllers, the steady error of the NDO–NTSMC is reduced by 40%, which effectively improves the tracking precision of the system. Therefore, the effectiveness of the NDO–NTSMC controller is verified.

With the concept of mean square value E(RMS) in mathematical statistics as a measure of the tracking error, the function is as follows:

$$E(e) = \left(\frac{1}{N} \sum_{i=1}^{n} e_i^2 \right)^{1/2} \tag{34}$$

where N is the total number of samples. Since the value of the desired trajectory is different from the angle of the robotic arm at beginning, this produces a large error. The sampling starts from 2.0 s, and the number of samples $N = 580$.

The result is shown in Table 2. Compared with NDO–PD, the E values of NDO–NTSMC are decreased by 79.2% and 88.6%, respectively, while compared with NTSMC, these values are decreased by 92.8% and 96.9%, respectively. It indicates the superiority of the NDO–NTSMC method in tracking accuracy. The simulation result verifies the effectiveness of the proposed controller.

Table 2. RMS of tracking errors using three different controllers.

Controller	Joint 1	Joint 2
NDO–NTSMC	0.0049	0.0017
NDO–PD	0.0236	0.0149
NTSMC	0.0677	0.0545

6. Conclusions

In this paper, a non-singular terminal sliding mode controller with disturbances observer has been raised for robotic manipulators trajectory tracking under model uncertainties and external disturbance. In particular, it can maintain an acceptable tracking effect when facing external time-varying disturbance. At the same time, the nonlinear sliding mode surface solves the singularity difficulty of the terminal sliding mode control. According to the Lyapunov function, it shows that the control system has the ability of global asymptotically stability. Finally, the availability of the NDO–NTSMC method has been proved by the simulation. This method also shows us that the complex of a disturbance observer and sliding mode controller is a promising direction, and it expands the practical application of sliding mode control theory. It should be noted that the method proposed in this article can also be promoted in other nonlinear uncertain MIMO systems such as unmanned aerial vehicles (UAVs) and humanoid robots.

Author Contributions: Conceptualization, K.G. and P.S.; methodology, writing—original draft preparation P.S.; validation, P.W.; software, writing—review and editing, C.H. and H.Z. All authors have read and agreed to the published version of the manuscript.

Funding: This research received no external funding.

Acknowledgments: The authors are very grateful to the reviewers, associate editors, and editors for their valuable comments and time spent.

Conflicts of Interest: The authors declare no conflict of interest.

References

1. Kreutz, K. On manipulator control by exact linearization. *IEEE Trans. Autom. Control* **1989**, *34*, 763–767. [CrossRef]
2. Poignet, P.; Gautier, M. Nonlinear model predictive control of a robot manipulator. In Proceedings of the 6th international workshop on advanced motion control, Nagoya, Japan, 30 March–1 April 2000.
3. Zhao, J.B.; Wang, X.Y.; Zhang, G.X. Design and implementation of membrane controllers for trajectory tracking of nonholonomic wheeled mobile robots. *Integr. Comput. Aided Eng.* **2015**, *23*, 15–30.
4. Hoo, S.; Xie, L.H.; Man, Z.H. Robust finite-time consensus tracking algorithm for multirobot systems. *IEEE/ASME Trans. Mechatron.* **2009**, *14*, 219–228.
5. Zhou, J.; Wen, C.Y.; Wang, W. Adaptive control of uncertain nonlinear systems with quantized input signal. *Automatica* **2018**, *95*, 152–162. [CrossRef]
6. Qureshi, M.S.; Swernkar, P.; Gupta, S. A supervisory on-line tuned fuzzy logic based sliding mode control for robotics: An application to surgical robots. *Robot. Auton. Syst.* **2018**, *109*, 68–85. [CrossRef]
7. Islam, S.; Liu, X.P. Robust sliding mode control for robot manipulators. *IEEE Trans. Ind. Electron.* **2010**, *58*, 2444–2453. [CrossRef]
8. Gao, D.X.; Xue, D.Y. Terminal Sliding Mode Adaptive Control for Robotic Manipulators. In Proceedings of the 6th World Congress on Intelligent Control and Automation, Dalian, China, 21–23 June 2006.
9. Utkin, V.; Guldner, J.; Shi, J. Sliding mode control in electromechanical systems. *Math. Probl. Eng.* **2009**, *8*, 451–473. [CrossRef]
10. Sabanovic, A. Variable structure systems with sliding modes in motion control-a survey. *IEEE Trans. Ind. Inf.* **2011**, *7*, 212–223. [CrossRef]
11. Fateh, M.M.; Aza, R.S. Discrete adaptive fuzzy control for asymptotic tracking of robotic manipulators. *Nonlinear Dyn.* **2014**, *78*, 2195–2204. [CrossRef]
12. Ang, L.Y.; Chai, T.Y.; Zhai, L.F. Neural network-based terminal sliding-mode control of robotic manipulators including actuator dynamics. *IEEE Trans. Ind. Electron.* **2009**, *56*, 3296–3304.
13. Cuong, P.; Wang, Y.N. Adaptive trajectory tracking neural network control with robust compensator for robot manipulators. *Neural Comput. Appl.* **2016**, *27*, 525–536. [CrossRef]
14. Wang, L.; Sheng, Y.Z.; Liu, X.D. A novel adaptive high-order sliding mode control based on integral sliding mode. *Int. J. Control. Autom. Syst.* **2014**, *12*, 459–472. [CrossRef]
15. Man, Z.H.; Paplinski, A.P.; Wu, H.R. A robust MIMO terminal sliding mode control scheme for rigid robotic manipulators. *IEEE Trans. Autom. Control.* **1994**, *39*, 2464–2469.
16. Yu, S.; Yu, X.; Shirinzadeh, B. Continuous finite-time control for robotic manipulators with terminal sliding mode. *Automatica* **2005**, *41*, 1957–1964. [CrossRef]
17. Feng, Y.; Yu, X.H.; Man, Z.H. Non-singular terminal sliding mode control of rigid manipulators. *Automatica* **2002**, *38*, 2159–2167. [CrossRef]
18. David, C.O.; Isaac, C.; Alexander, P. Non-singular terminal sliding-mode control for a manipulator robot using a barrier Lyapunov function. *ISA Trans.* **2022**, *121*, 268–283.
19. Wang, Y.Y.; Chen, J.W.; Yan, F.; Zhu, K.W.; Chen, B. Adaptive super-twisting fractional-order nonsingular terminal sliding mode control of cable-driven manipulators. *ISA Trans.* **2019**, *86*, 163–180. [CrossRef] [PubMed]
20. Yagiz, N.; Hacioglu, Y. Robust control of a spatial robot using fuzzy sliding modes. *Math. Comput. Model.* **2009**, *49*, 114–127. [CrossRef]
21. Jouila, A.; Nouri, K. An adaptive robust nonsingular fast terminal sliding mode controller based on wavelet neural network for a 2-DOF robotic arm. *J. Frankl. Inst.* **2020**, *357*, 13259–13282. [CrossRef]
22. Chen, W.H.; Balance, D.J.; Gawthrop, P.J. A nonlinear disturbance observer for two link robotic manipulators. In Proceedings of the 38th IEEE Conference on Decision and Control, Phoenix, AZ, USA, 6 August 2002; IEEE: Piscataway, NJ, USA.
23. Mohammadi, A.; Tavakoli, M.; Marquez, H.J. Nonlinear disturbance observer design for robotic manipulators. *Control. Eng. Pract.* **2013**, *21*, 253–267. [CrossRef]
24. Chen, W.H.; Balance, D.J.; Gawthrop, P.J. A nonlinear disturbance observer for robotic manipulators. *IEEE Trans. Ind. Electron.* **2000**, *47*, 932–938. [CrossRef]
25. Zheng, W.; Chen, M. Tracking Control of Manipulator Based on High-Order Disturbance Observer. *IEEE Access* **2018**, *6*, 26753–26764. [CrossRef]
26. Han, J.Q.; Wu, A.G.; Dong, N. Terminal sliding mode control for robotic manipulator based on sliding mode disturbance observer. *J. Cent. South Univ. (Sci. Technol.)* **2020**, *51*, 2749–2757.
27. Zhu, Y.; Wu, D.; Li, S. Non-singular Fast Terminal Sliding Mode Tracking Control of a 2-DOF Robotic Manipulator Using Finite-Time Extended State Observer. In Proceedings of the 2021 33rd Chinese Control and Decision Conference (CCDC), Kunming, China, 22–24 May 2021; IEEE: Piscataway, NJ, USA.